

## Thermodynamic Discontinuity between Low-Density Amorphous Ice and Supercooled Water

V. P. Shpakov,<sup>1,2,3,\*</sup> P. M. Rodger,<sup>1</sup> J. S. Tse,<sup>2</sup> D. D. Klug,<sup>2,†</sup> and V. R. Belosludov<sup>3</sup>

<sup>1</sup>Department of Chemistry, Warwick University, Coventry CV4 7AL, United Kingdom

<sup>2</sup>Steele Institute for Molecular Sciences, National Research Council of Canada, Ottawa, Canada K1A 0R6

<sup>3</sup>Institute of Inorganic Chemistry, Siberian Branch of Russian Academy of Science, Novosibirsk, Russia

(Received 24 November 2001; published 29 March 2002)

A combination of reverse Monte Carlo, molecular dynamics, and lattice dynamics simulations were used to obtain structural and thermodynamic data for low-density amorphous ice. A thermodynamically discontinuous transformation to a phase with properties and a structure consistent with supercooled liquid water is found to occur at  $\sim 130$  K. Quantum corrections have a profound effect on thermodynamic properties and the location of important thermodynamic points in the water phase diagram.

DOI: 10.1103/PhysRevLett.88.155502

PACS numbers: 61.43.Bn, 64.60.-i, 64.70.Kb, 67.80.Cx

The relationship between the structure of amorphous ices and the liquid water is of current interest since the thermodynamic properties of water in the important region below the melting point are not well understood. Several different scenarios are suggested including a second critical point [1], a retracing spinodal [2], and singularity free interpretations [3]. In the first proposal, it is suggested that below the second postulated critical point (ca.  $T = 220$  K and  $P = 1$  kbar), there would exist two liquid phases: a low-density liquid (LDL) and high-density liquid (HDL) [1]. The pressure amorphized phase of ice (HDA) and the phase prepared by annealing HDA at 120 K (LDA) are considered in this hypothesis as the corresponding glassy states of HDL and LDL. However, there are significant differences between LDA and hyperquenched glassy water (HQW) in their kinetic and thermodynamic behavior [4]. Recent Raman spectroscopic studies [5] and incoherent inelastic neutron scattering data [6] show that hydrogen bonding interactions in LDA differ from those in HQW. These facts, and also the different mechanism identified for the formation of HDA from *Ih* ice [7], led to questions about the thermodynamic connection between the amorphous ices and liquid phases of water.

To gain better insight for this problem reliable microscopic simulations are required. There are serious difficulties with generating model amorphous ice structures by supercooling the liquid [8] or compressing hexagonal ice *Ih* [9] due to the long relaxation time. Reverse Monte Carlo (RMC) analysis of experimental data may yield imperfect results since this method takes into account only the structural agreement of static positions of molecules without energetic considerations [10]. In this Letter we describe how this problem can be minimized through the use of RMC to obtain starting configurations of LDA and then relaxation using molecular dynamic (MD) and lattice dynamic (LD) calculations.

All calculations on LDA ice were started from a model structure consisting of 1536 water molecules obtained from the experimental structure factors using RMC [11] and subsequently were optimized with a conjugate-gradient method employing a modified TIP4P potential

for water. This potential gives improved calculated crystal unit cell parameters for various phases of ice [12], gives structural data in reasonable agreement with experimental data for LDA at 77 K [13], and yields good values for the enthalpy difference between ice *Ic* and ices II and IX at 150 K (60 and 320 J/mol, respectively, compared with the experimental values of 54 and 358 J/mol [14]). The final optimized LDA structure (model I) has a calculated potential energy of  $-51.3$  kJ/mol. This is 4 kJ/mol higher than the potential energy of *Ic* ice ( $-55.3$  kJ/mol). The calculated energy difference (4 kJ/mol), however, is much larger than the experimental enthalpy difference of 1.35–1.5 kJ/mol between supercooled water and ice *Ic* at 150 K [15]. Given the accuracy of the modified TIP4P potential in reproducing the energy of ice II and IX, we suspect that this discrepancy may in fact be connected with structural differences between LDA and supercooled water. To test this possibility, model I was used as the starting structure for MD/LD calculations to subsequently obtain the equilibrium LDA structures.

MD simulations were performed using Berendsen's constant temperature-pressure (NPT) method in a DL\_POLY package [16], with 0.25 fs time steps, an Ewald summation for electrostatic interactions, and with thermostat/barostat relaxation times of 1 ps. MD equilibration typically took 500–1250 ps and the same code was used in LD calculations for quenched configurations as in previous studies [7,11].

A practical scheme for including both quantum and anharmonic effects is to combine classical MD with quantum effects obtained from the quasiharmonic approximation [17]. This approach has been tested on a Lennard-Jones solid [17] and shown to be competitive with the predictions of effective-potential Monte Carlo and is in very good agreement with path-integral Monte Carlo results. Berens *et al.* [18] used a similar approach to study liquid water by pure MD techniques. We employ here the quasiharmonic lattice dynamics method [19] to estimate the quantum effects on the pressure and the structure of LDA. For this purpose, NPT MD calculations were first performed at  $T = 77$  K and at five different pressure points in the

density region 0.92–0.96 g/cm<sup>3</sup>. The quasiharmonic quantum correction to the free energy  $\Delta F$  can be evaluated from the following relation [17]:

$$\Delta F = \beta^{-1} \sum_k \ln \left( 2 \sinh \left[ \frac{1}{2} \beta \hbar \omega_k \right] \right) - \beta^{-1} \sum_k \ln(\beta \hbar \omega_k), \quad (1)$$

where  $\beta = \frac{1}{kT}$  and  $\omega_k$  is the frequency of the  $k$ th normal mode.  $\Delta F$  was calculated by the LD method in a number of the local minima and then averaged over these minima to deduce the volume dependence of  $\Delta F$ . The quantum correction to the pressure was then calculated by numerical differentiation of  $\Delta F$  with respect to volume, and the temperature dependence was estimated directly from the quenched configurations using Eq. (1). The results are presented in Fig. 1, together with the calculated values for Ic ice for comparison. The quantum pressure corrections were found to be surprisingly large (4.0 kbar at  $T = 77$  K) and approximately independent of density.

Radial distribution functions (RDFs) have also been obtained including quantum effects. A set of configurations was taken from an MD simulation, quenched, and then used in LD calculations. RDFs were calculated for every configuration by thermodynamical averaging of the operator

$$\rho(\hat{r}) = \frac{1}{N \rho_0 4\pi r^2 dr} \int_r^{r+dr} \sum_{k,k'} \delta(r' - r_{kk'}) dr' \quad (2)$$

over the appropriate canonical distribution function where  $\rho_0$  is the average density,  $N$  is the number of molecules in the simulation, and  $r_{kk'}$  is the instantaneous distance between atoms  $k$  and  $k'$ .

The effect of averaging is to replace the delta function with a Gaussian where the half-widths can be determined

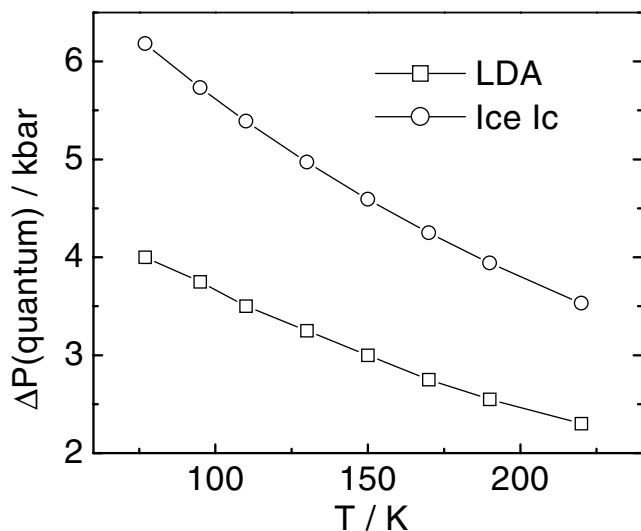


FIG. 1. Quantum correction to the classical MD pressure for LDA and Ic structures in the temperature range 70–220 K.

from the eigenvectors and eigenvalues of the harmonic Hamiltonian [20]. The RDFs were then averaged over the set of quenched configurations. A series of *NPT* MD simulations were then performed at zero total pressure for temperatures of 77, 95, 110, 130, 140, and 150 K. Given the quantum corrections, the simulations were actually performed at negative classical pressures of –4.0, –3.75, –3.5, –3.25, –3.13, and –3.0 kbar, respectively. For each temperature 50 configurations were taken from the last 250 ps of the trajectory by sampling every 5 ps. These instantaneous structures were energy minimized and quenched using a conjugate gradient method. In Fig. 2 the temperature dependence of the potential energy averaged over the quenched and instantaneous structures is shown. In the latter case, the thermal contribution to the potential energy ( $3RT$  for a rigid water molecule, where  $R$  is the gas constant) has been subtracted to give a classical estimate of the quenched potential energy. The two methods typically agree to within 0.1 kJ/mol.

Figure 2 shows that the potential energy of the model system decreases as temperature increases. There is an apparent discontinuity in the range 110–130 K which suggests that a phase transition occurs in this temperature range. The transition is identified as from the relaxed LDA structure at  $T = 77$  K (quenched to give structural model II) to a new amorphous structure at  $T = 150$  K (quenched to give structural model III). To verify this proposal, additional MD simulations were performed, starting from structural model III and lowering the temperature to 77 K. The results showed that the transition was not reversible on the MD time scale, and there is also an underlying free energy difference,  $\Delta F$ , between structures II and III of 0.65 kJ/mol, with state III giving the lower free energy at 77 K.

Quantum corrected RDF calculations are presented in Fig. 3. The distinct peaks in the calculated neutron RDF for model II and their intensities at 1.8, 2.3, 2.8, 3.2, 3.9,

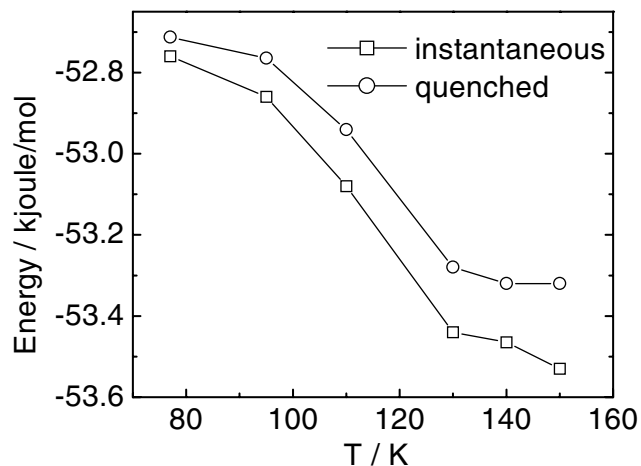


FIG. 2. Potential energy of quenched and instantaneous structures at various temperatures. Individual points are the potential energy in kJ/mol averaged over LD calculations on 50 quenched configurations.

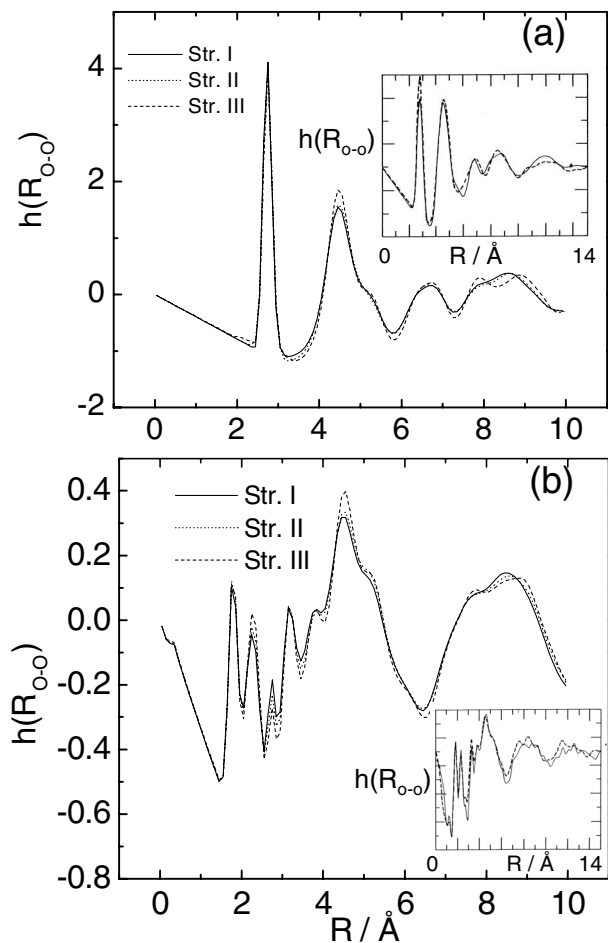


FIG. 3. (a) The weighted O-O pair correlation function for structures I, II, and III compared with experimental results for LDA (inset) [13]; (b) comparison of experimental total pair correlation function, extracted from neutron scattering study (inset) [13], with that calculated for structures I, II, and III. In the insets, the solid and dashed lines are for HQW and LDA ice, respectively.

and 4.5 Å as well as the shoulder at 5.1 Å and broad peak between 7 and 10 Å are in excellent agreement with the result (inset of Fig. 3b) derived from experimental data [13]. There are small but subtle structural differences between models II and III which are very similar to those observed experimentally between LDA and HQW (inset of Fig. 3b). In particular, the small intensity differences of the peaks at 2.8, 3.2, and 4.5 Å are comparable with those in the experimental data. In addition, the broad peak between 7 and 10 Å is shifted to slightly higher distances for model III compared with model II, as is seen in the RDFs for LDA and glassy water. The calculated RDF for O atoms (Fig. 3a) is also in good agreement with the experimental result (inset in Fig. 3a). The first two peaks in models II and III, corresponding to the first and second neighbor O atoms, are calculated at 2.75 and 4.5 Å compared with the experimental values of 2.8 and 4.6 Å, respectively. There is also a shoulder at 5.2 Å in the calculated RDF that is apparent in the experimental RDF for glassy water. The two broad peaks calculated at  $\sim 6.8$  and

$\sim 9$  Å are very close to the experimental result, including evidence for slightly more structure on the latter peak in glassy water.

The simulated structures were analyzed to determine the coordination number distribution for model I and averaged from the 50 quenched configurations taken from models II and III. These results are summarized in Table I along with results [21] for supercooled liquid water. It is instructive to examine the number of four-coordinated water molecules that have only four-coordinated neighbors up to their  $i$ th neighbor and these are presented in Table II. The results reveal a strong similarity between model III and the supercooled liquid. In contrast, model II has a lower percentage of four-coordinated water molecules ( $\sim 92\%$ ) than model III ( $\sim 96.5\%$ ) and a more rapid decay in the density of four-coordinate neighbors. Note that the calculated free energy difference of 0.65 kJ/mol between models II and III again agrees very well with the 0.5 kJ/mol reported for the free energy difference between LDA and amorphous water obtained from the analysis of experimental data [4]. In addition, the calculated enthalpy (1.7 kJ/mol) and free energy (1.45 kJ/mol) difference between model III and ice Ic at  $T = 150$  K are in reasonable agreement with the corresponding experimental values of 1.35–1.5 kJ/mol and 1.0–1.2 kJ/mol, respectively [22]. It is significant that the calculated density of structure II ( $0.94 \text{ g/cm}^3$ ) agrees with experimental density of LDA ( $0.94 \pm 0.2 \text{ g/cm}^3$ ). The calculated diffusion constant of model III at 150 K is  $6 \times 10^{-9} \text{ cm}^2/\text{s}$  and is in good agreement with an extrapolation of the value calculated for supercooled water at 193 K [23]. The small change of energy with temperature for structural model III is similar to that calculated at higher temperatures [24] and typical for a strong liquid. Therefore, we can reasonably assert that structural models II and III have distinct characteristics and can be identified as LDA ice and supercooled water, respectively.

The calculated density of model III at 150 K ( $0.93 \text{ g/cm}^3$ ) appears lower than that calculated in [24] for the supercooled liquid at 193 K ( $0.975 \text{ g/cm}^3$ ). This difference can be attributed to the neglect of quantum corrections in [24]: including quantum corrections, the former simulations are actually performed at a much higher pressure—ca. 2.5 kbar at 220 K (see Fig. 1)—than ambient. The experimental analysis suggests a second critical point

TABLE I. Coordination number distribution  $p_i$  (% of waters having  $i$  neighbors).

Structure	$i$				
	2	3	4	5	6
Supercooled liquid					
233 K (Ref. [21])	1	11	83	5	0
193 K (Ref. [21])	0	3	95	2	0
LDA					
Str. I	0	12	82	6	0
Str. II	0	5	92	3	0
Str. III	0	2.5	96.5	1	0

TABLE II. Percentage of water molecules which have only four coordinated neighbors up to  $i$ th neighbors.

Structure	$i$			
	0	1	2	3
Supercooled liquid				
233 K (Ref. [21])	83	44	8	0
193 K (Ref. [21])	95	80	50	20
LDA				
Str. I	82	40	6	0
Str. II	92	69	30	5
Str. III	96.5	86	62	29

in the water phase diagram occurs at 230 K and 0.5 kbar [25], while MD simulations [24] suggest it could be at negative pressures (between  $-2$  kbar and ambient). The difference is the same magnitude as the quantum pressure corrections, and so the discrepancy may simply be due to the neglect of quantum effects in [24].

The comparatively high probability of four-coordinated water molecules in the LDA structure suggests a higher degree of local ordering and the fairly structured RDF indicates significant long-range ordering. The higher degree of ordering in this system should imply sound excitations will have longer lifetimes than is usual in other glass-forming materials. This is consistent with a recent experimental observation by inelastic x-ray scattering of sharp phononlike excitations in LDA [26].

In summary, using a realistic configuration obtained from a RMC and a combination of molecular dynamics, energy minimization, and lattice dynamics, we found that the relative energies and structural features strongly resemble those of observed supercooled liquid water. From the heating of model LDA, a phase transition to a liquid structure is predicted at about 130 K. Analysis showed that their structural differences agree with those between experimental LDA and HQW. We concluded from the structural changes and clear energetic difference between model structures that the supercooled water is a distinct phase and not a continuation of LDA ice. Furthermore, we demonstrate that quantum effects play a significant role in the thermodynamic properties of LDA ice.

This work was supported by NATO/Royal Society, by the Russian Fund for Basic Research (Grant No. 00-03-32508), and by the NCERC. Computer time was provided under EPSCRC Grant No. GR/M91624.

\*Present address: The Angstrom Laboratory, Inorganic Chemistry Department, Uppsala University, Box 538, S-751 21 Uppsala, Sweden.

†Authors to whom correspondence should be addressed.

- [1] P.H. Poole, F. Sciortino, U. Essman, and H.E. Stanley, *Nature (London)* **360**, 324 (1992).
- [2] S. Sastry, P.B. Debenedetti, F. Sciortino, and E. Stanley, *Phys. Rev. E* **53**, 6144 (1996).
- [3] R.J. Speedy, *J. Phys. Chem.* **86**, 982 (1982).
- [4] G.P. Johari, *J. Chem. Phys.* **112**, 8573 (2000).
- [5] C.A. Tulk, D.D. Klug, R. Branderhorst, P. Sharpe, and J.A. Ripmeester, *J. Chem. Phys.* **109**, 8478 (1998).
- [6] D.D. Klug, C.A. Tulk, E.C. Svensson, and C.-K. Loong, *Phys. Rev. Lett.* **83**, 2584 (1999).
- [7] J.S. Tse, D.D. Klug, C.A. Tulk, I. Swainson, E.C. Svensson, C.-K. Loong, V. Shpakov, V.R. Belosludov, R.V. Belosludov, and Y. Kawazoe, *Nature (London)* **400**, 647 (1999).
- [8] P.H. Poole, U. Essman, F. Sciortino, and E.H. Stanley, *Phys. Rev. E* **48**, 4605 (1993).
- [9] I. Okabe, H. Tanaka, and K. Nakanishi, *Phys. Rev. E* **53**, 2638 (1996).
- [10] L. Pusztai, *Phys. Rev. B* **61**, 28 (2000).
- [11] J.S. Tse, D.D. Klug, C.A. Tulk, E.C. Svensson, I. Swainson, V.P. Shpakov, and V.R. Belosludov, *Phys. Rev. Lett.* **85**, 3185 (2000); D.D. Klug, J.S. Tse, C.A. Tulk, E.C. Svensson, I. Swainson, and C.-K. Loong, in *Science and Technology of High Pressure* (Universities Press Ltd., Hyderabad, 2000).
- [12] V.R. Belosludov, V.P. Shpakov, J.S. Tse, R.V. Belosludov, and Y. Kawazoe, *Ann. N.Y. Acad. Sci.* **912**, 993 (2000). The TIP4P has been improved by introducing a constant  $K = 1.0066$ . Partial charges are scaled by  $K^2$ ; the Lennard-Jones  $\sigma$  parameters are scaled by  $K^1$  and  $\epsilon$  by  $K^3$ ; finally, all distances between the interacting centers on the water molecule are scaled by  $K^1$ .
- [13] M.-C. Bellissent-Funel, L. Bosio, A. Hallbrucker, E. Mayer, and Sridi-Dorbez, *J. Chem. Phys.* **97**, 1282 (1992).
- [14] Y.P. Handa, D.D. Klug, and E. Whalley, *Can. J. Chem.* **66**, 919 (1988).
- [15] M.A. Floriano, Y.P. Handa, D.D. Klug, and E. Whalley, *J. Chem. Phys.* **91**, 7187 (1989).
- [16] W. Smith and T.R. Forester, *J. Mol. Graphics* **14**, 136 (1996).
- [17] R.J. Hardy, D.J. Lacks, and R.C. Shukla, *Phys. Rev. B* **57**, 833 (1998).
- [18] P.H. Berens, D.H. Mackay, G.M. White, and K.R. Wilson, *J. Chem. Phys.* **79**, 2375 (1983).
- [19] N.L. Allan, G.D. Barrera, R.M. Fracchia, M. Yu. Lavrentiev, M.B. Taylor, I.T. Todorov, and J.A. Purton, *Phys. Rev. B* **63**, 094203 (2001).
- [20] A.A. Maradudin, E.W. Montroll, G.H. Weiss, and I.P. Ipatova, *Theory of Lattice Dynamics in the Harmonic Approximation* (Academic Press, New York and London, 1971).
- [21] H. Tanaka, *Phys. Rev. Lett.* **80**, 113 (1998).
- [22] R.J. Speedy, P.G. Debenedetti, R. Scott Smith, C. Huang, and B.D. Kay, *J. Chem. Phys.* **105**, 240 (1996).
- [23] H. Tanaka, *J. Chem. Phys.* **105**, 5099 (1996).
- [24] H. Tanaka, *Nature (London)* **380**, 328 (1996).
- [25] O. Mishima, *Phys. Rev. Lett.* **85**, 334 (2000).
- [26] H. Schober, M.M. Koza, A. Tolle, C. Masciovecchio, F. Sette, and F. Fujara, *Phys. Rev. Lett.* **85**, 4100 (2000).